FoG 2005/03

Dynamic rewiring in small world networks

J P L Hatchett,[1] N S Skantzos,[2] and T Nikoletopoulos[3]

[1]*Laboratory for Mathematical Neuroscience,*

RIKEN Brain Science Institute, Saitama 351-0198, Japan[*]

[2]*Instituut voor Theoretische Fysica, Celestijnenlaan 200D, K.U.Leuven B-3001, Belgium*[†]

[3]*Department of Mathematics, King's College London, Strand WC2R 2LS, U.K.*[‡]

arXiv:cond-mat/0508250v1 [cond-mat.dis-nn] 10 Aug 2005

Abstract

We investigate equilibrium properties of small world networks, in which both connectivity and spin variables are dynamic, using replicated transfer matrices within the replica symmetric approximation. Population dynamics techniques allow us to examine order parameters of our system at total equilibrium, probing both spin- and graph-statistics. Of these, interestingly, the degree distribution is found to acquire a Poisson-like form (both within and outside the ordered phase). Comparison with Glauber simulations confirms our results satisfactorily.

[*]Electronic address: hatchett@brain.riken.jp

[†]Electronic address: Nikos.Skantzos@fys.kuleuven.be

[‡]Electronic address: theodore@mth.kcl.ac.uk

I. INTRODUCTION

Small worlds are systems characterized by a local neighborhood (given by short-range bonds) with a sparse set of long-range connections per spin. This simple architectural effect has been shown to bring about remarkable cooperative and synchronization phenomena. The term 'small-world' has been coined by the now famous experiment by the Harvard social psychologist Stanley Milgram [1]: in 1967, as part of his research on the network of acquaintances in the United States, he took a number of letters and handed them over to people totally unrelated with the addressees, and, with the instructions to pass them over to someone they think might know the addressee. This process was repeated until the letters finally arrived to their destination. Stanley Milgram then estimated the average path length from the two randomly chosen individuals which turned out to be a mere six. This experiment revealed that although social networks are very sparse, in reality any two pair of nodes can be topologically very close. In fact, numerical studies of other types of real networks (e.g. citation, linguistic, disease spreading, etc) show that the small-world effect is a common architecture among real network structures and brings about optimal information processing. The question then arises, how do networks spontaneously evolve from (almost) random configurations into particular structures such as small-world ones? And which underlying process drives the distribution of the long-range short-cuts within the nodes? The above questions fall under a particularly active area of research, namely the evolution of networks (see e.g. [2, 3], or [4], for a recent review). Since real networks (be it biological, social, economic or otherwise) hardly ever maintain a static architecture this problem of predicting network structure has important applications. In this paper we attempt to formulate and describe the thermodynamics of the problem from an analytic point of view. This carries the obvious set of advantages and disadvantages: while resulting in robust and exact results, it will be amenable to a set of (perhaps not fully realistic) assumptions. To be precise, we examine a coupled system on a small-world architecture in which both nodes and connections are mobile. However, the two dynamic processes occur on distinct timescales; connections are assumed to evolve slowly enough such that, at each of their update steps, spins have effectively reached equilibrium. This will allow us to avoid solving the explicit dynamical relations and instead turn directly to the thermodynamics. Our starting point is the free energy per connection degree of freedom. We couple the two dynamic processes of the spins and the connections by constructing two Hamiltonians: a typical Ising one describing the energy of the spins and a Hamiltonian of the connections, constructed

to reward network configurations minimizing the free energy of the spins. This choice allows us to proceed analytically while retaining a sufficient amount of realism. The result is a replica theory where the replica dimension represents the ratio between the two temperatures (of the spins vs connection processes).

Our paper is organised as follows: In the following section we introduce our model and the pair of energy functions describing the thermodynamics of the spins and the graph variables. In section III we write the total free energy of the system as an extremisation problem in terms of the typical finite-connectivity order parameter function. We then proceed to define the observables of our system, of which there are here two kinds, probing spin (section IV A) and graph (section IV B) organization statistics respectively. The single pure state approximation (section V) allows us to deal with the resulting replicated transfer matrices following the diagonalization process of [5, 6]. We first derive in section V A numerically tractable forms for our set of order functions which are to be solved via population dynamics. Observables such as magnetization, average connectivity, or degree distribution then follow easily, see section V B. We perform a bifurcation analysis and plot phase diagrams showing the transition lines between ordered and paramagnetic phases in section V C. We find that, perhaps contrary to initial expectations, the resulting degree distributions are close to, or exactly, Poisson. Comparison with numerical simulations shows good agreement given the complexity of these experiments requiring adiabatic (practically infinitely long) timescales.

II. MODEL DESCRIPTION

We study a system of N Ising spins $\boldsymbol{\sigma} = (\sigma_1, \ldots, \sigma_N)$ with $\sigma_i \in \{-1, 1\}$, arranged on a "small-world" structure. We represent this by a one-dimensional lattice with uniform nearest-neighbor interactions of strength J_0 and with randomly-chosen sparse short-cuts of strength $J_{ij} \in \{-J, J\}$ that can connect distant pairs of spins (i, j). For every $i \neq j$ we assign a variable c_{ij} denoting whether a connection exists ($c_{ij} = 1$) or not ($c_{ij} = 0$), with $c_{ii} = 0$. In the absence of short-cuts the average path length is $N/4$ while in the combined system the scaling is bounded above by $\log(N)$. This significant reduction in the path length is commonly termed the "small-world" effect [7]. For static architectures, in which the link and bond matrices $\{c_{ij}, J_{ij}\}$ are taken as quenched random variables, frustration effects are known to induce spin-glass phases [6]. Our model aims to examine thermodynamic properties of the above spin systems under the freedom of allowing the connectivity

and bond matrices $\{c_{ij}, J_{ij}\}$ to evolve in time in search of the state that best promotes order within the system. To be precise, on short timescales the links and bonds can be seen as static variables with respect to which the spins equilibrate, while on longer timescales c_{ij} and J_{ij} explore their configuration space. The measure of this latter process is related to the ordering within the spin system on the instantaneous state of the graph. Thus the spins and the graph architecture on which they live are dynamically interwoven. It is quite natural that the architecture dynamics depends on the entire system state (including the spins) rather than just the architecture itself (as with e.g. preferential attachment [8]). Links and connectivities are taken here to evolve on identical timescales, although generalizing this to more involved scenarios is also possible. On the timescale in which spins reach thermal equilibrium our combined system is described by the "fast" Hamiltonian

$$H_f(\boldsymbol{\sigma}, \boldsymbol{c}, \boldsymbol{J}) = -J_0 \sum_i \sigma_i \sigma_{i+1} - \sum_{i \leq j} \sigma_i J_{ij} c_{ij} \sigma_j \tag{1}$$

(where we take periodic boundary conditions on the chain). Spins equilibrate with respect to (1) at an inverse temperature $1/\beta_f$, and their behavior is described by the partition function

$$Z_f(\boldsymbol{c}, \boldsymbol{J}) = \sum_{\boldsymbol{\sigma}} \mathrm{e}^{-\beta_f H_f(\boldsymbol{\sigma}, \boldsymbol{c}, \boldsymbol{J})} \tag{2}$$

On timescales sufficiently long to guarantee that spins have reached equilibrium, links and bonds are not static, but evolve dynamically and we will take their stationary state to be described by the "slow" Hamiltonian

$$H_s(\boldsymbol{c}, \boldsymbol{J}) \;=\; -\frac{1}{\beta_f} \log Z_f(\boldsymbol{c}, \boldsymbol{J}) + V(\boldsymbol{c}, \boldsymbol{J}) \tag{3}$$

$$V(\boldsymbol{c}, \boldsymbol{J}) \;=\; \frac{1}{\beta_s} \sum_{i<j} c_{ij} \left[\log\left(\frac{N}{c}\right) + \log\cosh(K_p) - K_p \frac{J_{ij}}{J} \right] \tag{4}$$

This choice energetically favors those configurations of $\{c_{ij}, J_{ij}\}$ that minimize the free energy of the spins. The role of the chemical potential $V(\boldsymbol{c}, \boldsymbol{J})$ is twofold: firstly, it aims to preserve the overall nature of the small-world system; it guarantees that for $N \to \infty$ the average number of connections per spin is a finite number. Secondly, it allows us to tune the relative concentration of $\{-J, J\}$ bonds in the system (as we will see in section IV B, the former is controlled by the variable c whereas the latter by K_p). The connectivity- and bond-variables $\{c_{ij}, J_{ij}\}$ equilibrate with respect to this slow Hamiltonian at inverse temperature β_s, leading to a total partition function

$$Z_s = \sum_{\boldsymbol{c}, \boldsymbol{J}} \mathrm{e}^{-\beta_s H_s(\boldsymbol{c}, \boldsymbol{J})} = \sum_{\boldsymbol{c}, \boldsymbol{J}} [Z_f(\boldsymbol{c}, \boldsymbol{J})]^{\beta_s/\beta_f} \; \mathrm{e}^{-\beta_s V(\boldsymbol{c}, \boldsymbol{J})} \tag{5}$$

This partition function, by construction, contains $n = \beta_s/\beta_f$ replicas of the fast system. In general, the ratio of inverse temperatures n can take any value (integer or otherwise) so that analytic continuation in the replica dimension depends solely on our choice of temperature values. The limit $n \to 0$ corresponds to temperatures $T_s \to \infty$ in which the partition sum (5) is dominated by the entropy of the slow system. In contrast, $T_s \to 0$ favors those architectures $\{c_{ij}, J_{ij}\}$ that increase order among the spin variables for a given number of links. Note that this is a general optimization criterion which does not enforce *a priori* any particular structure on the links but allows the links to arrange themselves. In fact, the graph statistics become interesting observables, which we can measure, rather than enforced constraints. Our order parameters follow from the slow free energy per spin

$$f_s = -\lim_{N\to\infty} \frac{1}{\beta_s N} \log Z_s \tag{6}$$

and derivatives of this generating function.

III. THE FREE ENERGY

To calculate the slow partition function (5) we first take the trace over the connectivity and bond variables $\{c_{ij}, J_{ij}\}$

$$Z_s = \sum_{\boldsymbol{\sigma}_1 \ldots \boldsymbol{\sigma}_N} \mathrm{e}^{\beta_f J_0 \sum_i \boldsymbol{\sigma}_i \cdot \boldsymbol{\sigma}_{i+1}} \prod_{i<j} \left[1 + \frac{c}{N} \left\langle \mathrm{e}^{\beta_f J \boldsymbol{\sigma}_i \cdot \boldsymbol{\sigma}_j} \right\rangle_J \right] \tag{7}$$

up to irrelevant multiplicative constants. We denote $\boldsymbol{\sigma}_i = (\sigma_i^1, \ldots, \sigma_i^n)$ where $\boldsymbol{\sigma}_i \cdot \boldsymbol{\sigma}_j = \sum_\alpha \sigma_i^\alpha \sigma_j^\alpha$ and defined the abbreviation $\langle f(J) \rangle_J = [2\cosh(K_p)]^{-1}[e^{K_p} f(J) + e^{-K_p} f(-J)]$. We are interested in the case where c (the chemical potential for bonds) is finite, and hence $c/N \to 0$ in the limit $N \to \infty$, so that the above product can alternatively be seen as a product over exponentials (up to terms of $\mathcal{O}(N^{-2})$). We thus encounter the typical nested exponential form of finite connectivity problems. To achieve site factorization it is convenient to introduce into our expressions the order parameter function [9, 10]

$$P(\boldsymbol{\sigma}) = \frac{1}{N} \sum_i \delta_{\boldsymbol{\sigma}, \boldsymbol{\sigma}_i} \tag{8}$$

via appropriately defined delta functions, which is a probability distribution over replicated spins. In the limit $N \to \infty$ we can now evaluate the free energy (6) via steepest descent and express it as

an extremization problem in the space of probability distributions $P(\boldsymbol{\sigma})$, namely:

$$f_s \;=\; \mathrm{extr}_{\{P(\boldsymbol{\sigma})\}}\left\{\frac{c}{2\beta_s}\sum_{\boldsymbol{\sigma}\boldsymbol{\sigma}'}P(\boldsymbol{\sigma})P(\boldsymbol{\sigma}')\left\langle \mathrm{e}^{\beta_f J\boldsymbol{\sigma}\cdot\boldsymbol{\sigma}'}\right\rangle_J - \lim_{N\to\infty}\frac{1}{\beta_s N}\log\sum_{\boldsymbol{\sigma}_1\ldots\boldsymbol{\sigma}_N}\prod_i T_{\boldsymbol{\sigma}_i,\boldsymbol{\sigma}_{i+1}}[P]\right\}$$

where $T_{\boldsymbol{\sigma},\boldsymbol{\sigma}'}[P]$ represent the transfer matrix elements

$$T_{\boldsymbol{\sigma},\boldsymbol{\sigma}'}[P] = \exp\left[\beta_f J_0\boldsymbol{\sigma}\cdot\boldsymbol{\sigma}' + c\sum_{\boldsymbol{\tau}}P(\boldsymbol{\tau})\left\langle \mathrm{e}^{\beta_f J\boldsymbol{\sigma}\cdot\boldsymbol{\tau}}\right\rangle_J\right] \tag{9}$$

and $P(\boldsymbol{\sigma})$ is to be evaluated from the fixed-point equation

$$P(\boldsymbol{\sigma}) = \frac{\mathrm{Tr}\left(Q[\boldsymbol{\sigma}]\,T^N[P]\right)}{\mathrm{Tr}\left(T^N[P]\right)} \qquad Q_{\boldsymbol{\sigma},\boldsymbol{\sigma}'}[\boldsymbol{\tau}] \equiv \delta_{\boldsymbol{\sigma},\boldsymbol{\tau}}\delta_{\boldsymbol{\sigma},\boldsymbol{\sigma}'} \tag{10}$$

For more details on the derivation of the above expressions we refer the reader to [6] where the special case of the $n \to 0$ limit was studied.

Finding solutions of (10) amounts to diagonalising the transfer matrix T of dimensionality $2^n \times 2^n$. This problem has been solved in [5]. Here we will not be concerned in the entire spectrum of eigenvalues, as the limit $N \to \infty$ ensures that only the largest eigenvalue λ_0 will provide a non-vanishing contribution to the free energy. The left- and right- eigenvectors associated with this eigenvalue follow from the equations

$$\sum_{\boldsymbol{\sigma}'} T_{\boldsymbol{\sigma},\boldsymbol{\sigma}'}[P]\; U(\boldsymbol{\sigma}') = \lambda_0\; U(\boldsymbol{\sigma}) \tag{11}$$

$$\sum_{\boldsymbol{\sigma}'} V(\boldsymbol{\sigma}')\; T_{\boldsymbol{\sigma}',\boldsymbol{\sigma}}[P] \;= \lambda_0\; V(\boldsymbol{\sigma}) \tag{12}$$

These eigenvectors are unique up to the usual arbitrary multiplicative factor, and non-negative [5, 11]. We note that we need both left- and right-eigenvectors since the transfer matrix $T[P]$ is non-symmetric. The order function $P(\boldsymbol{\sigma})$ (8) is manifestly normalized. Due to our scaling freedom for the eigenvectors we can always choose them so that $\sum_{\boldsymbol{\sigma}} U(\boldsymbol{\sigma}) = \sum_{\boldsymbol{\sigma}} V(\boldsymbol{\sigma}) = 1$. The physics of our system is given by the normalized distributions $P(\boldsymbol{\sigma})$, $V(\boldsymbol{\sigma})$, $U(\boldsymbol{\sigma})$ which are to be found by self-consistently solving equations (9-12) (in fact, $U(\boldsymbol{\sigma})$ and $V(\boldsymbol{\sigma})$ turn out to represent the distributions of cavity spins with a chain bond rather than a graph bond removed [11]).

IV. OBSERVABLES

A. Spin system observables

We are interested in probing organizational properties of our system both within the spin variables and the connectivity ones. For the spin system, we define the canonical observables; the magnetization and the overlap order parameter as moments of the probability distribution (8), namely

$$m_\alpha \;=\; \sum_{\boldsymbol{\sigma}} P(\boldsymbol{\sigma})\; \sigma^\alpha \tag{13}$$

$$q_{\alpha\beta} \;=\; \sum_{\boldsymbol{\sigma}} P(\boldsymbol{\sigma})\; \sigma^\alpha \sigma^\beta \tag{14}$$

In the above and henceforth, the quantities $P(\boldsymbol{\sigma})$, $V(\boldsymbol{\sigma})$, $U(\boldsymbol{\sigma})$ are given by their saddle-point values.

It is well known that infinite dimensional systems, such as small world lattices, with frozen bonds of random signs, will have a spin-glass ground state at low temperatures for certain values of the control parameters [12, 13, 14]. This spin glass ordering is intimately linked to frustration within the system; the inability of spins to find energetically optimal configurations. By allowing the architecture some limited degree of freedom, we expect that the system will be able to optimize its state somewhat better. Probing the degree of frustration within the system as the slow temperature is varied is therefore an interesting problem. The frustration is normally defined as the fraction of closed loops from sites $i_1 \to i_2 \to \ldots i_k \to i_1$ where the product $J_{i_1 i_2} \ldots J_{i_k i_1}$ is negative. Unfortunately, to measure this directly in our system where bonds are mobile would require us to be able to measure correlations over long length scales within the system (in fact scaling like the average loop length $\sim \log(N)$), which is technically difficult. To try and finesse this problem, in [15, 16], the fraction of misaligned spins was calculated, i.e. the fraction of spins that did not point in the direction of their local field. Due to the mobility of the connections in our system we expect that thermal equilibrium states within the ordered phases will be steered towards configurations where spin alignment with their local fields is optimal. The result of this structural organization can be measured by the following quantity $\phi = \int_{-\infty}^{0^-} \mathrm{d}h\, P(1,h) + \int_{0^+}^{\infty} \mathrm{d}h\, P(-1,h)$ which gives the fraction of misaligned spins and is defined in terms of the joint spin-field distribution $P(\sigma,h) = \lim_{N\to\infty} \frac{1}{N} \sum_i \langle \delta_{\sigma,\sigma_i} \delta[h - h_i(\boldsymbol{\sigma})] \rangle_{\mathrm{s}}$ where $\langle \cdots \rangle_{\mathrm{s}}$ denotes thermal averages over the slow process $\langle x \rangle_{\mathrm{s}} = Z_s^{-1} \sum_{\boldsymbol{c},\boldsymbol{J}} e^{-\beta_s H_s(\boldsymbol{c},\boldsymbol{J})} x$ and $h_i(\boldsymbol{\sigma}) \equiv \sum_j c_{ij} J_{ij} \sigma_j + J_0(\sigma_{i+1} + \sigma_{i-1})$ denotes the local field at site i. However, at e.g. very low temperatures, one expects the spins to align to their local fields whether they are in a spin glass phase

or not. Thus to try and get a different measure to probe the frustration in the system we consider the fraction of bonds in the graph, which are not energetically optimized by the spin configuration:

$$\psi = \frac{1}{N}\sum_i \langle \Theta(-\sigma_i\sigma_{i+1}J_0)\rangle_{\rm s} + \frac{1}{cN}\sum_{i<j}\langle c_{ij}\Theta(-\sigma_i\sigma_j J_{ij})\rangle_{\rm s} \tag{15}$$

This is also not an absolute measure of frustration, but in the low temperature spin glass phase ψ will be non-zero, as opposed to a low temperature ferromagnet where we would have $\psi = 0$. The calculation of either ψ or ϕ is similar to the calculation of the free-energy, with a specific observable (i.e. matrix in the transfer matrix notation) at one or two sites. We find

$$\psi = D_1 \sum_{\boldsymbol{\sigma}\boldsymbol{\sigma}'} V(\boldsymbol{\sigma})\Theta(-\sigma_1\sigma_1' J_0) T_{\boldsymbol{\sigma}\boldsymbol{\sigma}'}[P]U(\boldsymbol{\sigma}') + D_2 \sum_{\boldsymbol{\sigma}\boldsymbol{\sigma}'} P(\boldsymbol{\sigma})P(\boldsymbol{\sigma}')\langle \Theta(-\sigma_1\sigma_1' J) {\rm e}^{\beta_f J \boldsymbol{\sigma}\cdot\boldsymbol{\sigma}'}\rangle_J \tag{16}$$

where D_1 and D_2 are normalization constants to give the fraction of sites, i.e. $D_1 = \sum_{\boldsymbol{\sigma}\boldsymbol{\sigma}'} V(\boldsymbol{\sigma}) T_{\boldsymbol{\sigma}\boldsymbol{\sigma}'}[P]U(\boldsymbol{\sigma}')$ and $D_2 = \sum_{\boldsymbol{\sigma}\boldsymbol{\sigma}'} P(\boldsymbol{\sigma})\, P(\boldsymbol{\sigma}')\left\langle e^{\beta_f J \boldsymbol{\sigma}\cdot\boldsymbol{\sigma}'}\right\rangle$.

B. Connectivity system observables

Let us now inspect organisational phenomena within the graph. We first identify the roles played by the control parameters c and K_p that appear in the chemical potential (4). This can be done by adding suitable generating terms into the Hamiltonian (3) and monitoring their impact on (9). For instance, if one transforms $H_s \to H_s + \lambda \frac{1}{c}\sum_{i<j} c_{ij}$ then taking derivatives $\frac{\partial f_s}{\partial \lambda}|_{\lambda=0}$ translates to

$$\overline{c} \equiv \frac{1}{N}\sum_{ij}\langle c_{ij}\rangle_{\rm s} = c\sum_{\boldsymbol{\sigma}\boldsymbol{\tau}} P(\boldsymbol{\sigma})\, P(\boldsymbol{\tau})\, \left\langle {\rm e}^{\beta_f J \boldsymbol{\sigma}\cdot\boldsymbol{\tau}}\right\rangle_J \tag{17}$$

Now $\overline{c}$ represents the average number of connections per spin in our system. It depends on the replica dimension n via the scalar spin product and it reduces to $\overline{c} = c$ in the limit $n \to 0$. In the limit $c \to \infty$ (scaling J as J/c to keep the local fields in the graph $h_i^{\rm gr}(\boldsymbol{\sigma}) \equiv \sum_j c_{ij}J_{ij}\sigma_j$ of $\mathcal{O}(1)$) we again recover $\overline{c} = c$ to leading order as found in [15]. Similarly to the above, one also finds that taking $H_s \to H_s + \lambda \sum_{i<j} c_{ij}J_{ij}$ produces the average bond strength on the graph. As well as being interested in the above average connectivity and bond strength at total equilibrium, we would also like to investigate the connectivity structure in more detail. To make contact with a variety of recent work on complex networks [4, 19] we define the degree distribution for our system

$$\Xi(k) = \lim_{N\to\infty}\frac{1}{N}\sum_i \left\langle \delta_{k,\sum_j c_{ij}}\right\rangle_{\rm s} \tag{18}$$

Following a calculation similar to that of the free energy in section III one easily finds that

$$\Xi(k) \sim \int \frac{\mathrm{d}\hat{k}}{2\pi}\, \mathrm{e}^{ik\hat{k}} \sum_{\boldsymbol{\sigma}\boldsymbol{\sigma}'} V(\boldsymbol{\sigma})U(\boldsymbol{\sigma}')\, \exp[c \sum_{\boldsymbol{\tau}} \langle P(\boldsymbol{\tau})\, \mathrm{e}^{\beta_f J \boldsymbol{\sigma}\cdot\boldsymbol{\tau} - \mathrm{i}\hat{k}} \rangle_J + \beta_f J_0 \boldsymbol{\sigma}\cdot\boldsymbol{\sigma}'] \tag{19}$$

The above observables are all expressed in terms of the trio of distributions $P(\boldsymbol{\sigma})$, $V(\boldsymbol{\sigma})$ and $U(\boldsymbol{\sigma})$, taken at the saddle-point of the free energy (9). To proceed with a numerical evaluation of the observables one now needs to specify a form for these.

V. REPLICA SYMMETRY AND TRANSFER-MATRIX DIAGONALISATION

To solve the self-consistent equation (10) one is required to make certain assumptions. Firstly with regards to the form of the order function $P(\boldsymbol{\sigma})$ and the eigenvectors. They represent different distributions over replicated spins (for any $n \in \mathbb{R}$). We will consider the simplest possible scenario in which permutation of spins within different replica groups $\alpha = 1, \ldots, n$ leave the order function invariant (replica symmetry). This is equivalent to assuming the existence of a single pure state.

For any natural $n \in \mathbb{N}^+$ it is relatively straightforward to express these distributions, as their support is a finite discrete set. However, for the more general case of $n \in \mathbb{R}$ one has to make an analytic continuation which leads to more complicated expressions.

For any natural n we can impose replica symmetry by writing for any arbitrary distribution $X(\boldsymbol{\sigma})$

$$X(\boldsymbol{\sigma}) = \sum_{\ell=0}^{n} \mathcal{X}(\ell)\ \delta[2\ell - n; \sum_{\alpha} \sigma_\alpha] \tag{20}$$

where normalisation of $X(\boldsymbol{\sigma})$ requires $\sum_{\ell=0}^{n} \mathcal{X}(\ell)\binom{n}{\ell} = 1$. On the other hand, for any real n

$$X(\boldsymbol{\sigma}) = \int \mathrm{d}z\ x(z)\ \prod_{\alpha=1}^{n} \frac{e^{z\sigma_\alpha}}{[2\cosh(z)]} \tag{21}$$

where now normalization requires $\int \mathrm{d}z\, x(z) = 1$. The above ansätze hold for any distribution $X(\boldsymbol{\sigma})$, and in particular as $X \in \{P, U, V\}$ we define the natural n ansätze in terms of $\{\mathcal{P}, \mathcal{U}, \mathcal{V}\}$ and for real n in terms of $\{p, u, v\}$ respectively.

A. Self-consistent order function equations

Our self-consistent equations for P, U, V (10-12) can now be transformed into relations between the field distributions $\{\mathcal{P}, \mathcal{U}, \mathcal{V}\}$ or $\{p, u, v\}$. Let us start with the natural n versions. It is conve-

nient to begin by working out an identity for the replica symmetric form of the general expression $\sum_{\boldsymbol{\sigma}} X(\boldsymbol{\sigma})F(\boldsymbol{\sigma}\cdot\boldsymbol{\tau})$. We insert the replica symmetric ansatz (20) for X, use the gauge transformation $\sigma_\alpha \to \sigma_\alpha\tau_\alpha$ and introduce the representation of unity $1 = \sum_{k=0}^{n}\delta[2k-n;\sum_\alpha \tau_\alpha]$ which results in

$$\sum_{\boldsymbol{\sigma}} X(\boldsymbol{\sigma})F(\boldsymbol{\sigma}\cdot\boldsymbol{\tau}) = \sum_{\ell=0}^{n}\sum_{k=0}^{n}\mathcal{X}(\ell)\delta[2k-n;\sum_\alpha\tau_\alpha]\sum_{\boldsymbol{\sigma}}\delta[2\ell-n;\sum_\alpha\sigma_\alpha\tau_\alpha]F(\sum_\alpha\sigma_\alpha) \tag{22}$$

We now define the set of replica indices $S=\{\alpha\in\{1,\ldots,n\}:\tau_\alpha=1\}$ and its complement $\overline{S}=\{\alpha\in\{1,\ldots,n\}:\tau_\alpha=-1\}$ which allows us to write $\sum_\alpha\tau_\alpha\sigma_\alpha=\sum_{\alpha\in S}\sigma_\alpha-\sum_{\alpha\in\overline{S}}\sigma_\alpha$. Isolating these last two summations via the unities $1=\sum_{k_1=0}^{k}\delta[2k_1-k;\sum_{\alpha\in S}\sigma_\alpha]$ and $1=\sum_{k_2=0}^{n-k}\delta[2k_2+k-n;\sum_{\alpha\in\overline{S}}\sigma_\alpha]$ and using the general identity $\sum_{\sigma_1\ldots\sigma_p}\delta[2q-p;\sum_{\alpha=1}^{p}\sigma_\alpha]=\binom{p}{q}$, we obtain

$$\begin{aligned}\sum_{\boldsymbol{\sigma}} X(\boldsymbol{\sigma})F(\boldsymbol{\sigma}\cdot\boldsymbol{\tau}) = &\sum_{\ell,k=0}^{n}\sum_{k_1=0}^{k}\sum_{k_2=0}^{n-k}\mathcal{X}(\ell)\,\delta[2k-n;\sum_\alpha\tau_\alpha]\\ &\times\delta[\ell+k+k_2-k_1-n;0]\,F(2(k_1+k_2)-n)\binom{k}{k_1}\binom{n-k}{k_2}\end{aligned} \tag{23}$$

Using the above identity (and very similar manipulations) we can write our self-consistent equations as

$$\mathcal{U}(\ell) \;=\; \lambda_0^{-1}(n)\,\exp[cA_P(\ell,J)]\,A_U(\ell,J_0) \tag{24}$$

$$\mathcal{V}(\ell) \;=\; \lambda_0^{-1}(n)\sum_{j=0}^{n}\sum_{k_1=0}^{j}\sum_{k_2=0}^{n-j}\mathcal{V}(j)\,\mathrm{e}^{cA_P(j,J)+\beta_f J_0[2(k_1+k_2)-n]}\,\delta[\ell+j+k_2-k_1-n;0] \tag{25}$$

$$\mathcal{P}(\ell) \;=\; \frac{\mathcal{U}(\ell)\,\mathcal{V}(\ell)}{\sum_{\ell=0}^{n}\binom{n}{\ell}\mathcal{U}(\ell)\,\mathcal{V}(\ell)} \tag{26}$$

The largest eigenvalue $\lambda_0(n)$ follows from the above by utilizing the normalization condition $\sum_\ell\binom{n}{\ell}\mathcal{U}(\ell)=1$. We have introduced the convenient shorthand,

$$A_X(\ell,J)=\sum_{i=0}^{n}\sum_{j=0}^{\ell}\sum_{k=0}^{n-\ell}\mathcal{X}(i)\;\delta[i+k+\ell-j-n;0]\;\binom{\ell}{j}\binom{n-\ell}{k}\langle\mathrm{e}^{\beta_f J[2(j+k)-n]}\rangle_J \tag{27}$$

for $X\in\{P,U,V\}$ and $\mathcal{X}\in\{\mathcal{P},\mathcal{U},\mathcal{V}\}$ respectively.

Let us now turn to the more general case of $n\in\mathbb{R}$. Firstly, a Taylor expansion of the transfer matrix elements (9) into a series of exponentials and insertion of the replica symmetric ansatz (21) leads to

$$T_{\boldsymbol{\sigma},\boldsymbol{\sigma}'}[P]=\mathrm{e}^{\beta_f J_0\boldsymbol{\sigma}\cdot\boldsymbol{\sigma}'}\left\langle\mathrm{e}^{\beta_f\theta\sum_\alpha\sigma_\alpha}\right\rangle_\theta \tag{28}$$

with $\langle\cdots\rangle_\theta$ representing averages over the measure

$$M(\theta|n)=\sum_{k\geq 0}\frac{\mathrm{e}^{-c}c^k}{k!}\left\langle\int[\prod_{l\leq k}\frac{\mathrm{d}h_l\,p(h_l)}{[2\cosh(h_l)]^n}]\;\mathrm{e}^{n\sum_l B(J_l,h_l)}\;\delta[\theta-\sum_{l\leq k}A(J_l,h_l)]\right\rangle_{\{J_l\}} \tag{29}$$

and where we introduced the functions

$$A(J,x) \;=\; \mathrm{atanh}(\tanh(\beta_f J)\tanh(x)) \tag{30}$$

$$B(J,x) \;=\; \frac{1}{2}\log\left[4\cosh[\beta_f J+x]\cosh[\beta_f J-x]\right] \tag{31}$$

The first of the above functions can be identified as a 'message' (or effective field) passed during belief propagation while the latter is related to the free energy shifts which occur during an iteration [14, 17]. For $n\to 0$ and within replica symmetry this second term does not contribute although in the more general case of $n>0$ it will play an important role. Following the belief propagation picture, one can also relate (29) to a weighted measure over the messages coming from the long range bonds. Performing the spin summations in (11-12) using the ansatz (21) and requiring the resulting expression to have the eigenvector form leads to

$$\lambda_0(n)\;u(x|n) \;=\; \int \mathrm{d}x'\;u(x'|n)\;\frac{\cosh^n(x)}{\cosh^n(x')}\left\langle \mathrm{e}^{nB(J_0,x')}\delta[x-\theta-A(J_0,x')]\right\rangle_\theta \tag{32}$$

$$\lambda_0(n)\;v(y|n) \;=\; \int \mathrm{d}y'\;v(y'|n)\;\frac{\cosh^n(y)}{\cosh^n(y')}\left\langle \mathrm{e}^{nB(J_0,y'+\theta)}\delta[y-A(J_0,y'+\theta)]\right\rangle_\theta \tag{33}$$

so that the largest eigenvalue follows from the above by simple integration. To close the above equations we also need to derive an expression for the function $p(h)$. The starting point for this is equation (10). Rewriting the traces in terms of the eigenvectors and substituting our ansatz (21) results in

$$p(h)=\frac{\int \mathrm{d}x\,\mathrm{d}y\;u(x)\,v(y)\;\left\{\frac{\cosh(h)}{2\cosh(x)\cosh(y)}\right\}^n\;\delta[h-(x+y)]}{\int \mathrm{d}x\,\mathrm{d}y\;u(x)\,v(y)\left\{\frac{\cosh(x+y)}{2\cosh(x)\cosh(y)}\right\}^n} \tag{34}$$

The coupled set of equations (32,33,34) are to be solved self-consistently. This has a clear interpretation in terms of message-passing algorithms: $p(h)$ gives the distribution of messages passed along long-range short-cuts, whereas, $u(x)$ and $v(y)$ that of messages passed along the chain (from the left- and right- neighbors). This inspires a solution using a population dynamics methodology [17]; the main difference is that one is now required to weight the averages of the field distributions by an n-dependent factor. In practice, expressions of the form $\phi(x')=\int \mathrm{d}x\,\phi(x)\,w(x)\;\delta[x'-g(x)]$

(for some arbitrary probability density $\phi(x)$, weight $w(x)$ and updating function $g(x)$) are solved by sampling values of x from the density $\phi(x)$ and updating $x' \to g(x)$ with weight $w(x)$. To interpret this weighting term, one can write $w(x) = \lfloor w(x) \rfloor + p$, where, $\lfloor w(x) \rfloor$ is the integer part of $w(x)$, and p is the fractional part. At each iteration step we replace $\lfloor w(x) \rfloor$ of the population members with x' and a further member with probability p.

B. Observables within replica symmetry

To calculate the magnetization (13) and spin glass (14) order parameter within our system, we substitute the replica symmetric ansatz for $P(\boldsymbol{\sigma})$ (20) into their definitions, which together with a minor rearrangement gives for integer n

$$m = \sum_{\ell=1}^{n} \mathcal{P}(\ell) \binom{n-1}{\ell-1} - \sum_{\ell=0}^{n-1} \mathcal{P}(\ell) \binom{n-1}{\ell} \tag{35}$$

$$q = \sum_{\ell=2}^{n} \mathcal{P}(\ell) \binom{n-2}{\ell-2} + \sum_{\ell=0}^{n-2} \mathcal{P}(\ell) \binom{n-2}{\ell} - \sum_{\ell=1}^{n-1} \mathcal{P}(\ell) \binom{n-2}{\ell-1} \tag{36}$$

while for real n the expressions become:

$$m = \int \mathrm{d}h \; p(h) \; \tanh(h) \tag{37}$$

$$q = \int \mathrm{d}h \; p(h) \; \tanh^2(h) \tag{38}$$

So given $\mathcal{P}$ or p from the self-consistent equations, for either integer or real n, we may evaluate these order parameters. In figure 1 we plot the magnetization for two different values of n, and compare our results against simulation experiments. More details on the simulations are given in section V D, but we note here that these experiments are particularly time consuming due to the coupled dynamics, so that, only modest system sizes are allowed for reasonable CPU cost. Within these constrains we feel that the agreement is reasonable.

Evaluating the fraction of energetically non-optimal bonds ψ is slightly more involved. We use the replica symmetric representation of the transfer matrix which for integer n reads

$$T_{\boldsymbol{\sigma},\boldsymbol{\sigma}'}[P] = \sum_{k=0}^{n} \delta(2k-n; \sum_{\alpha} \sigma^{\alpha}) \; \mathrm{e}^{\beta_f J_0 \boldsymbol{\sigma}\cdot\boldsymbol{\sigma}' + c A_P(k,J)} \tag{39}$$

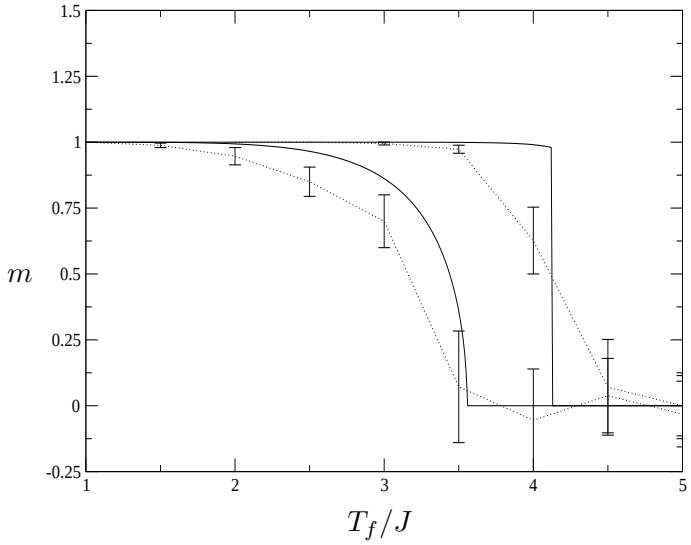

FIG. 1: We plot the magnetization m as a function of temperature T_f for $n = 1$ and $n = 5$. The solid lines are the theoretical predictions while the dotted lines are a guide for the eye joining the markers with error bars which come from simulations. We have $c = 2$ and $J_0 = J_{ij} = 1\ \forall i, j$. The simulations were done via Monte Carlo Glauber dynamics (see text for details) on $N = 200$ spins. Despite the small system size they seem to be in reasonable agreement with the theory.

Then, after some combinatorial work, ψ is found to be given by

$$\begin{aligned}
\psi \;=\; & D_1 \sum_{i=1}^{n}\sum_{j=0}^{n-1}\sum_{k=0}^{i-1} \mathrm{e}^{\beta_f J_0(2k-j-1)} \binom{n-1}{i-1}\binom{i-1}{k}\binom{n-i}{j-k}\left\{\mathcal{V}(i)\mathcal{U}(j)\mathrm{e}^{cA_P(i,J)} + \mathcal{V}(j)\mathcal{U}(i)\mathrm{e}^{cA_P(j,J)}\right\} \\
& + D_2 2p \sum_{i=1}^{n}\sum_{j=0}^{n-1}\sum_{k=0}^{i-1} \mathcal{P}(i)\mathcal{P}(j)\binom{n-1}{i-1}\binom{i-1}{k}\binom{n-i}{j-k}\mathrm{e}^{\beta_f J(n+2(2k-i-j))} \\
& + D_2(1-p) \sum_{i=1}^{n}\sum_{j=1}^{n}\sum_{k=0}^{i-1} \mathcal{P}(i)\mathcal{P}(j)\binom{n-1}{i-1}\binom{i-1}{k}\binom{n-i}{j-k-1}\mathrm{e}^{\beta_f J(n+2(2k+1-i-j))} \\
& + D_2(1-p) \sum_{i=0}^{n-1}\sum_{j=0}^{n-1}\sum_{k=0}^{i} \mathcal{P}(i)\mathcal{P}(j)\binom{n-1}{i}\binom{i}{k}\binom{n-i-1}{j-k}\mathrm{e}^{\beta_f J(n+2(2k-i-j))}
\end{aligned} \tag{40}$$

For real n the replica symmetric transfer matrix is given by,

$$T_{\boldsymbol{\sigma},\boldsymbol{\sigma}'}[P] = \mathrm{e}^{\beta_f J_0 \boldsymbol{\sigma}\cdot\boldsymbol{\sigma}'} \int \mathrm{d}\theta M(\theta)\ \mathrm{e}^{\beta_f \theta \sum_\alpha \sigma_\alpha} \tag{41}$$

leading to

$$\begin{aligned}
\psi \;=\; & D_1 \int \mathrm{d}x\mathrm{d}y\mathrm{d}\theta\ u(x)v(y)M(\theta)\ \frac{\mathrm{e}^{-\beta_f J_0}\, 2\cosh(x+\theta-y)}{\left[\mathrm{e}^{y} 2\cosh(x+\theta+\beta_f J_0) + \mathrm{e}^{-y} 2\cosh(x+\theta-\beta_f J_0)\right]^{n-1}} \\
& + D_2 \int \mathrm{d}h_1\mathrm{d}h_2\ p(h_1)p(h_2)\ \mathrm{e}^{-\beta_f J}\ \frac{Q(J)2\cosh(h_1+h_2) + Q(-J)2\cosh(h_1-h_2)}{\left[\mathrm{e}^{h_2} 2\cosh(h+\beta_f J) + \mathrm{e}^{-h_2} 2\cosh(h-\beta_f J)\right]^{n-1}}
\end{aligned} \tag{42}$$

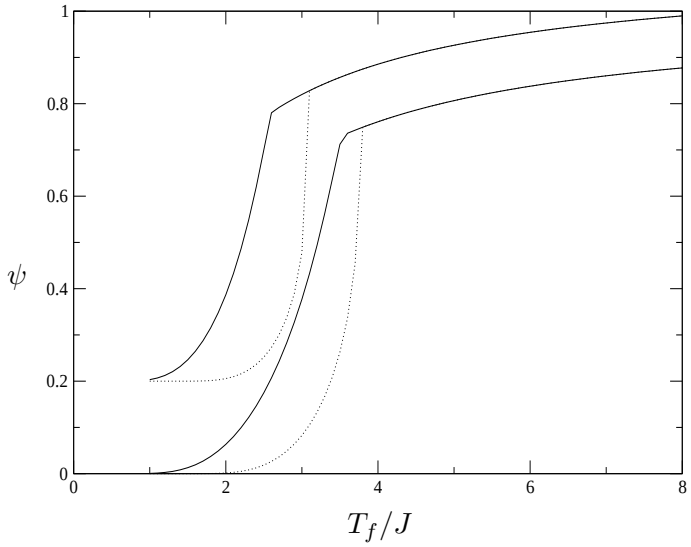

FIG. 2: We plot the fraction of misaligned bonds ψ against the re-scaled temperature T_f/J for $c = 2$ and $J_0 = 1$. The solid lines are for $n = 1$ while the dotted lines are for $n = 3$. The upper pair of lines are for $r = 0.8$ while the lower pair are for the ferromagnet, $r = 1$. We see that in the ordered phase, increasing n allows the system to optimize the bonds energetically.

where we define

$$Q(J') = r\delta_{J,J'} + (1-r)\delta_{-J,J'} \qquad r = \frac{\mathrm{e}^{K_p J}}{2\cosh(K_p J)} \tag{43}$$

We plot ψ for a few sets of parameters in figure 2. As the fast temperature goes to ∞ we have $\psi \to 1$, i.e. exactly half of the bonds at any point in time are energetically optimal, so in the high temperature phase the ordering is non-existent (as one would expect). We also see that increasing n leads to better levels of optimization, again what we would expect but it is possible to quantify it here. Decreasing r and hence increasing the disorder, makes it harder for the spins to energetically optimize themselves, although at low temperatures, due to the condensation phenomena in the bonds (see below), the magnetization will increase to 1. With all spins aligned, the fraction of energetically non-optimal bonds becomes exactly the fraction of bonds with $J < 0$. We see this in figure 2, as $T_f \to 0$, $\psi \to 1 - r$. This would not be the case for the pure spin-glass, $r = 0.5$.

We now turn our attention to the graph observables. We first focus on the average connectivity which is expressed as

$$\overline{c} = c \sum_k \mathcal{P}(k) A_P(k; J) \binom{n}{k} \tag{44}$$

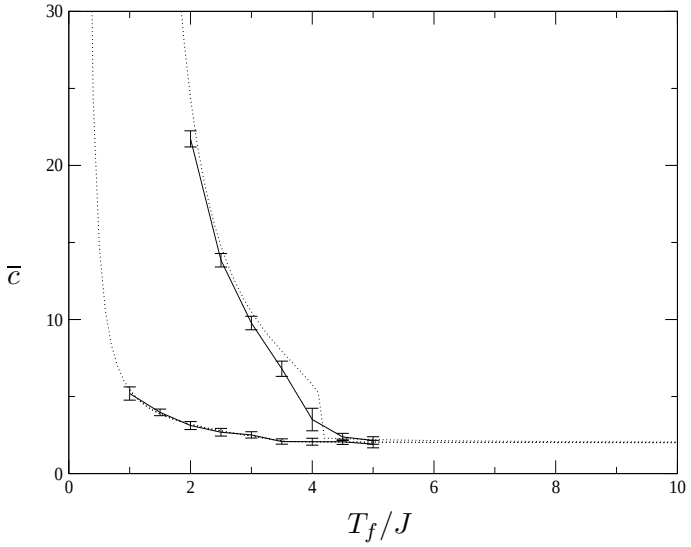

FIG. 3: We plot the average number of bonds $\overline{c}$ against temperature for $J = J_0 = 1$ and $c = 2$ in the ferromagnet. The higher line with the first order transition is for $n = 5$ while the lower line is for $n = 1$. The dotted lines are the theoretical predictions while the solid line is a guide for the eye linking the error bars which are measurements from simulation experiments. The agreement is reasonable although, as in fig. 1, we find that the sharp transition is smeared out due to the small system size for our simulations ($N = 200$ spins).

for integer n and

$$\overline{c} = c \int \mathrm{d}h_1 \, \mathrm{d}h_2 \; p(h_1) \, p(h_2) \;\; \{\cosh(\beta_f J) + \tanh(h_1) \tanh(h_2) \sinh(\beta_f J)\}^n \tag{45}$$

for real n.

If figure 3 we plot the average number of bonds $\overline{c}$. At low temperatures (the specific temperature depends on other parameters) the average connectivity increases sharply. This is due to ordering within the spin system leading to increased energetic gain by adding connections. Higher values of n, for a given T_f, means a lower value of T_s and hence the connectivity variables will be governed more strictly by the free energy of the fast system, which is minimized by high connectivity configurations.

We also looked at the full degree distribution, which is given up to normalization constants for integer n by

$$\Xi(k) \sim \frac{c^k}{k!} \sum_{i=0}^{n} \binom{n}{i} \; \mathcal{V}(i) \, \mathcal{U}(i) \; A_P^k(i, J) \tag{46}$$

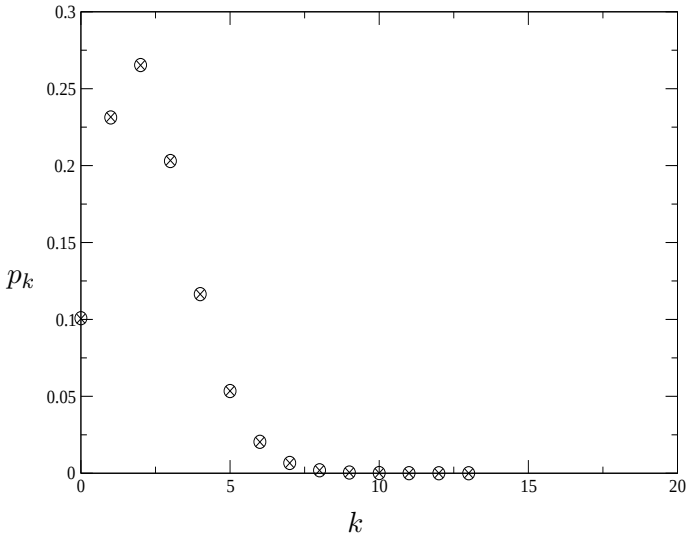

FIG. 4: We plot the probability that a given node has degree k, p_k against k for $n = 0.5$, $r = 0.6$, $T_f = J = J_0 = 1$ and $c = 2$ within the spin-glass regime where other observable values are $m = 0$ and $q \approx 0.581$. The true degree distribution is given by crosses, for comparison we have also given the Poisson distribution with the same value of $\overline{c}$ with circles. Although there are differences between the two for this set of parameters, the difference is very small.

and for real n by,

$$\Xi(k) \sim \frac{c^k}{k!} \int \prod_{\ell \leq k} \left\{ \frac{\mathrm{d}h_\ell \mathrm{d}J_\ell p(h_\ell) Q(J_\ell)}{[2\cosh(h_\ell)]^n} \right\} \frac{\mathrm{d}x \mathrm{d}y u(x) v(y)}{[4\cosh(x)\cosh(y)]^n} \mathrm{e}^{n\sum_\ell B(J_\ell,h_\ell)+nB(J_0,x)} \times \left\{ 2\cosh\left[y + A(J_0,x) + \sum_\ell A(J_\ell,h_\ell) \right] \right\} \tag{47}$$

A typical example of this degree distribution is given in figure 4. What is particularly interesting is that although the degree distribution is in principle free to take on any form it keeps very close to that of the Poisson degree distribution with mean $\overline{c}$. In fact in the paramagnetic phase, we know that $P(\boldsymbol{\sigma}) = 2^{-n}$ and thus we find $\overline{c}$ exactly from (17) without invoking replica symmetry, namely $\overline{c}_{PM} = c\cosh^n(\beta J)$, which is independent of r since cosh is an even function. Thus the average degree is independent of the bond disorder (in this model) in the paramagnetic phase. Here, the degree distribution also scales linearly with c. By using the fact that in the paramagnetic phase we also have $U(\boldsymbol{\sigma}) = V(\boldsymbol{\sigma}) = 2^{-n}$ we can also see that $\Xi(k) = \mathrm{e}^{-\overline{c}_{PM}} \overline{c}_{PM}^k / k!$, i.e. the degree distribution is exactly Poisson. We also find exact results in the fully ferromagnetic phase where $P(\boldsymbol{\sigma}) = U(\boldsymbol{\sigma}) = V(\boldsymbol{\sigma}) = \prod_\alpha \delta_{\sigma^\alpha,\sigma^1}$. There $\overline{c}_{FM} = c\langle \mathrm{e}^{\beta f nJ} \rangle_J$ and $\Xi(k) = \mathrm{e}^{-\overline{c}_{FM}} \overline{c}_{FM}^k / k!$. In both these

cases the degree distribution is exactly Poisson. We can understand this, since in both phases there is no energetic gain in having any particular $c_{ij} = 1$, since it will not affect the spin distribution (they are either all set to be aligned, or fully random) and thus the degree distribution will be the maximum entropy one, i.e. Poisson. It is also clear that there are a range of ordered states between the two extremes above, and that we cannot say anything further analytically about the degree distribution there. However, we may evaluate our order parameter equations numerically, and we find that although the degree distribution is not Poisson, it is very close, as shown in figure 4. It was not obvious that this should be the case, and indeed, the increased critical temperature for a scale free degree distribution would have suggested that this could be optimal, since it increases ordering, but it transpires that this is not the case here.

C. Phase diagrams

Having derived the main equations from which our observables follow, we can now proceed to the evaluation of the transition lines in our phase diagram numerically and via a bifurcation analysis. Firstly, we see that the state $p(x) = u(x) = v(x) = \delta(x)$ always solves equations (32,33,34), giving $m = q = 0$, for all temperatures. We can therefore associate this state with the high-temperature (paramagnetic) solution. To examine continuous bifurcations away from this solution we assume that close to the transition the fields are small and that the paramagnetic δ-distributions evolve to either distributions of small, non-zero mean (in leading order) marking the paramagnetic/ferromagnetic transition or to distributions of small, non-zero variance (again in leading order) marking the paramagnetic/spin-glass transition. With these considerations in mind we define the moments $\overline{h^\ell} = \int \mathrm{d}h\, p(h)\, h^\ell = \mathcal{O}(\epsilon^\ell)$ for some $0 < \epsilon \ll 1$ (and similarly for $\overline{x^\ell} = \int \mathrm{d}x\, u(x)\, x^\ell$ and $\overline{y^\ell} = \int \mathrm{d}y\, v(y)\, y^\ell$). We assume that there is no first order transition. Then, expanding equations (32,33,34) for small values of fields and using $\overline{h} = \overline{x} + \overline{y}$ and $\overline{h^2} = \overline{x^2} + \overline{y^2}$ which follows from (34) we arrive at paramagnetic/ferromagnetic and paramagnetic/spin-glass transition lines:

$$\mathrm{P} \to \mathrm{F}: \qquad 1 = c \left\langle \sinh(\beta_f J) \cosh^{n-1}(\beta_f J) \right\rangle_J \mathrm{e}^{2\beta_f J_0} \tag{48}$$

$$\mathrm{P} \to \mathrm{SG}: \qquad 1 = c \left\langle \sinh^2(\beta_f J) \cosh^{n-2}(\beta_f J) \right\rangle_J \cosh(2\beta_f J_0) \tag{49}$$

These equations reduce to those found in [6] in the limit $n \to 0$, recovering the small-world bifurcations. The correspondence is exact if we identify the paramagnetic mean connectivity here with

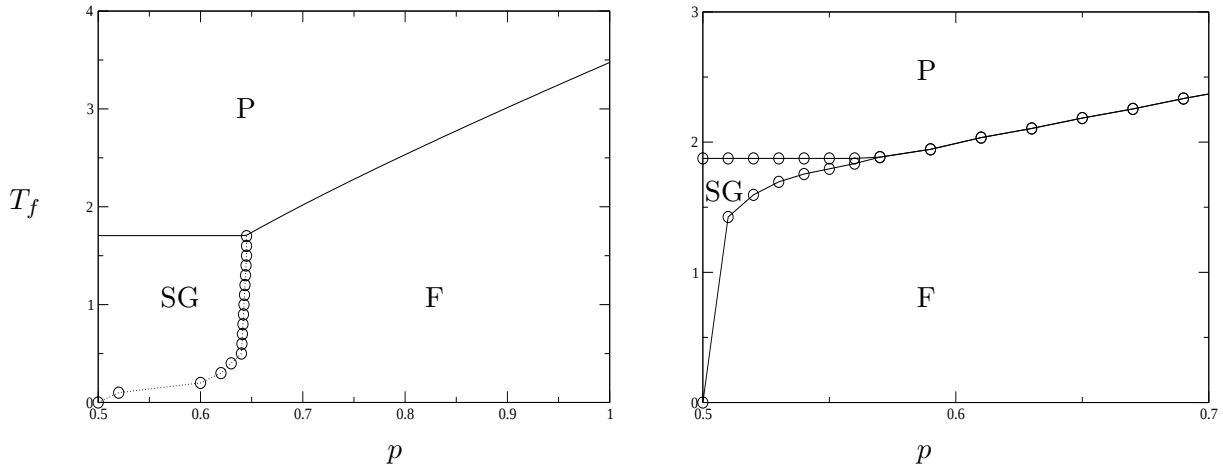

FIG. 5: We plot the phase diagrams for $c = 2$ and $J = J_0 = 1$. The left figure is for $n = 0.1$, where the solid lines are given by the bifurcation conditions (48,49) while the markers come from solving the order parameter equations numerically and the dotted line linking markers is a guide to the eye. The right figure is for $n = 2$ and all lines are linking markers which come from solving the order parameter equations numerically. The P→F and P→SG transitions are here first-order. For larger values of n we see that the links are better able to align to increase order; firstly, the transition temperature from the paramagnetic phase is higher and secondly, the size of the spin glass phase is significantly smaller.

c. It also reduces to those of [16] for $J_0 = 0$ and $Q(J') = \delta(J' - J)$, where the Hopfield model on a dynamic random graph was studied, if in the latter only a single pattern is stored (in this scenario the Hopfield model becomes equivalent to a ferromagnet with a different gauge). It is well known for these models [16] that as n increases, the transitions are increasingly likely to be first order. Thus to produce phase diagrams of the system, as well as looking at the bifurcation lines given by the above we also solved the full equations numerically. The results are shown in figure 5 where we see that increasing n decreases the size of the spin glass phase, which we expect is due to the increased cooperativity.

D. Simulations

In order to check the validity of our theoretical work we performed numerical simulations of this model. To do this we need to introduce a dynamical process on both the spins and the graph which will converge to an equilibrium distribution described by their respective Hamiltonians. One way to do this is via Glauber dynamics [18], the dynamics then automatically obey detailed balance. The transition rates between a given state and another state with a single "spin" flip (where we take spin in the broader sense to include the binary variables $\{c_{ij}\}$ and $\{J_{ij}\}$ as well as the more familiar $\{\sigma_i\}$) is determined by half the energy difference (or local field) between the two states. Defining general spin flip operators via $F^c_{ij}\Phi(c_{11}, c_{12}, \ldots, c_{NN}) = \Phi(c_{11}, c_{12}, \ldots, -c_{ij}, \ldots, c_{NN})$ and similarly for F^J_{ij} the Glauber rates can be written as

$$W[F^c_{ij}\mathbf{c}, \mathbf{c}] = \frac{1}{2}\left\{1 - \tanh\left[\frac{2c_{ij}-1}{2}\log\frac{c}{N} - \frac{n}{2}\log\langle \mathrm{e}^{-\beta_f(2c_{ij}-1)\sigma_i J_{ij}\sigma_j}\rangle\right]\right\} \tag{50}$$

$$W[F^J_{ij}\mathbf{J}, \mathbf{J}] = \frac{1}{2}\left\{1 - \tanh\left[J_{ij}K_p - \frac{n}{2}\log\langle \mathrm{e}^{-2\beta_f\sigma_i c_{ij} J_{ij}\sigma_j}\rangle\right]\right\} \tag{51}$$

where the angular brackets denote averages over the fast process for the given realization of the graph and bonds.

The nature of the coupled dynamics means that for each change to the graph (the slow dynamics) one must re-equilibrate the spins, measure the averages as required in the above equation and subsequently change the graph configuration again. Thus the computation effort required to equilibrate the slow system is very large compared to simulations on a given, fixed, graph. In particular, for strongly disordered graphs, where changing a single bond is expected to seriously alter the free-energy surface, it is very difficult to obtain reasonable statistics. Instead, we have focused our efforts on the simpler case of purely ferromagnetic bonds. This means that after changing a given bond, the new equilibrium distribution is expected to be very close to the old one and also the equilibration times will be shorter in general. We have performed simulations on systems with $N = 200$, and in figures 1 and 3 we compare the results with our theoretical predictions. Due to the small system size we must expect that there are both persistent errors due to the relatively small system size, smearing of all phase transitions and large error bars on any given measurement. Bearing this all in mind we feel that the results, particularly for the average connectivity, clearly support the theory.

VI. CONCLUSIONS

The study of complex networks has recently become a very popular field due to their ubiquity in nature, technology and social interaction, where these fields are meant in a broad sense. While the statistical structure characterizing real world networks (path lengths, degree distributions,...) and models that recreate these properties have been extensively studied from experimental measurements on real world systems, through numerical simulations and theory, understanding the behavior of networked systems based on local rules (dynamics) is still a relatively unexplored area [19]. We have presented a solvable model that examines a spin system on a small world graph with which we have probed cooperative behavior of the entire system (both of the graph and the spins). To overcome the theoretical challenge of systems evolving on disparate timescales we have focussed on the adiabatic limit; the graph evolves infinitely slowly relative to the spin variables. This allows us to treat the model using the well developed thermodynamics of replica theory, rather than having to treat the dynamics explicitly. The advantage of this approach is twofold. Firstly the results are exact in the thermodynamic limit in the region where replica symmetry is stable. Although we have not examined replica symmetry breaking experience suggests that this would only occur for $n < 1$, at low temperatures (high values of β_f) and for some critical amount of disorder in the bonds $\{J_{ij}\}$. The second benefit of this approach is related to the relative simplicity of our present approach. We do not specify in advance the dynamics of the graph, but instead only describe it through its equilibrium energy function. Thus the resulting graph structure becomes an observable itself, rather than an object which is fixed from the start. Indeed, naive intuition may suggest that the optimal structure could have been scale free, so that ordering in the spins would have occurred at a higher temperature. It turns out that this was not the case, apparently due to entropic reasons.

Acknowledgments

NSS wishes to warmly thank RIKEN Brain Science Institute for their kind hospitality during the final stages of this work and the Fund for Scientific Research Flanders-Belgium. We thank A C C

Coolen, I Pérez Castillo and B Wemmenhove for illuminating discussions.

---

[1] Milgram S (1967) *Psychology Today* **2** 60

[2] Barrat A, Barthélemy M, and Vespignani A (2004) *Phys Rev E* **70** 066149

[3] Chan DYC, Hughes BD, Leong AS, and Reed WJ (2003) *Phys Rev E* **68** 066124

[4] Dorogovtsev S N and Mendes J F F (2002) *Advances in Physics* **51** 1079-1187

[5] Nikoletopoulos T and Coolen A C C (2004) *J Phys A: Math Gen* **37** 8433

[6] Nikoletopoulos T, Coolen A C C, Pérez Castillo I, Skantzos N S, Hatchett J P L and Wemmenhove B (2004) *J Phys A* **37** 6455

[7] Watts D J and Strogatz S H (1998) *Nature* **393** 440

[8] Barabási A L and Albert R 1999 *Science* **286** 509

[9] Monasson R 1998 *J Phys A: Math Gen* **31** 513

[10] Wemmenhove B and Coolen A C C 2003 *J Phys A: Math Gen* **36** 9617

[11] Wemmenhove B, Nikoletopoulos T and Hatchett J P L 2004 `condmat/0405563`

[12] Viana L and Bray A J 1985 *J Phys C* **18** 3037

[13] Kanter I and Sompolinsky H 1987 *Phys Rev Lett* **58** 164

[14] Mezard M and Parisi G 1987 *Europhys Lett* **3** 1067

[15] Wemmenhove B, Skantzos N S and Coolen A C C 2004 *J Phys A: Math Gen* **37** 7653-7670

[16] Wemmenhove B and Skantzos N S 2004 *J Phys A: Math Gen* **37** 7843-7858

[17] Mézard M and Parisi G 2001 *Eur Phys J B* **20** 217

[18] Glauber R J 1963 *Jour Math Phys* **4** 294-307

[19] Newman M E J 2003 *SIAM Review* **45** 167-256